https://doi.org/10.17221/42/2022-CJGPB

# Transcriptome and proteome analysis of the fig (*Ficus carica* L.) cultivar Orphan and its mutant Hongyan based on the fruit peel colour in South China

*Lingzhu Wei, Jianhui Cheng, Jiang Xiang, Ting Zheng, Jiang Wu**

*Institute of Horticulture, Zhejiang Academy of Agricultural Sciences, Hangzhou, Zhejiang, P.R. China*

**Corresponding author: wujiang@zaas.ac.cn*

**Citation:** Wei L.Z., Cheng J.H., Xiang J., Zheng T., Wu J. (2023): Transcriptome and proteome analysis of the fig (*Ficus carica* L.) cultivar Orphan and its mutant Hongyan based on the fruit peel colour in South China. Czech J. Genet. Plant Breed., 59: 33–42.

**Abstract:** The external fruit colour is an important parameter of the fig fruit quality. Fig anthocyanin content is critical for the peel colour. The peel of mature fruits of the fig cultivar Orphan and its red peel bud mutant Hongyan were separated for a transcriptomic and proteomic analysis. A total of 162 different abundance proteins (DAPs) and 5 015 differentially expressed genes (DEGs) were identified. The correlation analysis revealed that only two and 15 genes were downregulated and upregulated, respectively, at both the transcriptome and proteome levels. The Kyoto Encyclopedia of Genes and Genomes (KEGG) analysis indicated that the enrichment pathways including Tropane, piperidine and pyridine alkaloid biosynthesis, phenylalanine metabolism and isoquinoline alkaloid biosynthesis for DEGs, and protein processing in the endoplasmic reticulum and flavonoid biosynthesis may contribute to the mutant color phenotype. Our results provide transcriptomic and proteomic information for two fig cultivars and may help to clarify the potential mechanisms of fig colouration.

**Keywords:** anthocyanin biosynthesis; fig (*Ficus carica* L.); fruit peel colour; proteomics; transcriptomics

The fig (*Ficus carica* L., *Moraceae*) is a traditional fruit tree. The fig is cultivated in most countries and regions of the world, especially in Mediterranean basin countries and California, the United States (Dueñas et al. 2008). Fig fruits have a very high safety profile. They have long been used to satisfy hunger and improve health. Fig fruits are rich in fibre and minerals, with little sodium or fat (Solomon et al. 2006; Crisosto et al. 2010). In addition, figs are rich in vitamins, such as thiamin (B1) and riboflavin (B2). Equally, dark colour figs contain high levels of phenolic compounds and have high antioxidant activities (Solomon et al. 2006).

In the world, there are more than 600 fig cultivars (Khadari et al. 1995), whose skin colour varies from green, yellow-green, or yellow to much deeper colours, such as red, purple and black. The development of fig fruits can be described as a double sigmoid growth curve (Marei & Crane 1971). During ripening, the fig fruit matures, and its colour changes when anthocyanins accumulate in the peel (Kislev et al. 2006). In general, the anthocyanin content depends on the cultivar and deeper-coloured skins contain higher levels of anthocyanins (Solomon et al. 2006).

Anthocyanins contribute to the colouration and play a vital role in the responses to external stress (Page et al. 2012). In addition, anthocyanins have an antioxidant capacity (Pascual-Teresa et al. 2010; Gowd et al. 2017).

There are two main stages in the anthocyanin biosynthetic pathway: the phenylpropanoid pathway and the flavonoid pathway. A series of primary enzymes

Supported by the Youth Talents Development Project in Zhejiang Academy of Agricultural Sciences (2016R05B).

https://doi.org/10.17221/42/2022-CJGPB

participate in these pathways, including phenylalanine ammonia lyase (PAL), cinnamate-4-hydroxylase (C4H), 4-coumaroyl: CoA-ligase (4CL), chalcone synthase (CHS), chalcone isomerase (CHI), flavanone 3-hydroxylase (F3H), flavonoid 3'-hydroxylase (F3'H), flavonoid 3',5'-hydroxylase (F3'5'H), dihydroflavonol 4-reductase (DFR), leucoanthocyanidin dioxygenase/anthocyanidin synthase (LDOX/ANS), and UDP-glucose: flavonoid 3-O-gluco-syltransferase (UFGT) (Tanaka et al. 2008; Wang et al. 2013). Additionally, several transcription factors have also been reported to play key roles in the biosynthesis of anthocyanins (Allan et al. 2008), including MYB transcription factors, basic helix-loop-helix (bHLH) proteins, and WD40 proteins (Höll et al. 2013).

The fig cultivar Orphan (Synonym: Jinaofen) with a yellow peel is highly cultivated in China. Hongyan is a bud mutant of the Orphan cultivar in which the fruit develops an appealing bright red colour when mature. These two studied cultivars had the same morphological characteristics, except for the peel colours.

The main objective of the present work is to understand the changes in the mutant fig cultivar and the potential pathway alterations involved in the fig peel colouration. We performed both transcriptome and proteome comparisons using the peel of the two cultivars.

## MATERIAL AND METHODS

**Plant material and treatment.** The fig cultivar Orphan and its bud mutant cultivar Hongyan were 4 years old and were grown under standardised cultivation and they were cultivated with 3 × 3 m spacing. They are conserved in the orchard of the Zhejiang Academy of Agricultural Science (120°24'E, 30°26'N), South China, at an altitude of 3.6 m a.s.l. The soil type is loamy paddy soil with a pH of 6.7. According to the UPOV (International Union for the Protection of New Varieties of Plants, Geneva, Switzerland, http://upov.int), there are few morphological differences between the two figs (e.g., globose and pyriform fruit shape, very large fruit width), except for the fruit colour when matured. The fig fruit were collected in the middle of phase III for the proteome, RNA-sequencing (RNA-Seq) and Real-Time Quantitative Reverse Transcription Polymerase chain reaction (qRT-PCR) analysis on September 18$^{th}$, 2017. Each fig's peel was excised at 2 mm thick and subsequently kept at –80 °C for future use.

**RNA extraction and transcript peel genome sequencing.** The cetyltrimethylammonium ammonium bromide (CTAB) method was applied to extract the total RNA from each sample as described previously (Chai et al. 2014). After the contaminating genomic DNA was removed, the total RNA was quantified with a NanoPhotometer Pearl (Implen, Germany) assay for the following experiments:

For the RNA-Seq, an Ultra™ RNA Library Prep Kit for Illumina (New England Biolabs, Inc., USA) was used to construct the cDNA libraries, and the raw read sequences were generated by Nanjing Vazyme Biotechnology Co. (Nanjing, China) using the Illumina HiSeqTM 2000 platform (Illumina, USA). The raw reads were then quality trimmed and assembled into contigs using the Trinity platform (Ver. 2.0.6). The gene expression values were calculated by the reads/fragments per kilobase of exon per million fragments mapped reads (RPKM/FPKM). Thresholds with a false discovery rate (FDR) ≤ 0.05 and a log2-fold change (FC) ≥ 1 were used to evaluate the significant difference. Due to the lack of published genome sequences (Mori et al. 2017), the obtained unigenes were used for BLASTX alignment. The RNA-seq data were deposited into the National Center for Biotechnology Information Sequence Read Archive (NCBI SRA) under accession number PRJNA730813.

**Real-time quantitative RT-PCR validation.** For the qRT-PCR analyses, *actin* was employed as the internal control. The qRT-PCR was performed using FastStart Universal SYBR Green (Roche, Basel, Switzerland), where the detailed qRT-PCR process was described in our previous report (Wei et al. 2020). Briefly, the extracted mRNA was reversely transcripted into cDNA using a PrimeScript RT Kit (TaKaRa, Japan). The PCR reaction was conducted on a CFX96 Real Time PCR Detection System (Bio-Rad, USA). The primers used in this study are listed in Table S1 in the Electronic Supplementary Material (ESM).

**Sample preparation and protein digestion.** The peel was ground using liquid nitrogen, followed by dissolution in a lysing solution, the protein was extracted using the method described previously with a few modifications (Zhao et al. 2019). The Bradford method was then carried out to detect the total protein concentration as previously described (Bradford 1976). Following digestion with trypsin, the peptides were desalted using a C18 column (100 μm × 20 mm, 3 μm, 100 Å, Thermo Fisher Scientific, Waltham,

https://doi.org/10.17221/42/2022-CJGPB

USA) and the desalted peptides were subsequently vacuum dried.

**Liquid chromatography-mass spectrometry analysis.** The LC-MS/MS analysis of the peptide sample was performed on a Q-Exactive HF-X MS platform (ThermoFisher Scientific). The peptide sequences were searched against our RNA-Seq data. Proteins with an FC ≥ 1.5 and $P \leq 0.05$ were considered significantly different.

**Statistical analysis.** The statistical significance between the two groups was calculated using Student's *t*-test in SPSS (Ver. 16.0, Chicago, USA) (Fiddler et al. 2011). The results are represented as the mean ± SD. GraphPad Prism 7 software (GraphPad Software, Ver. 2016) was used to construct the figures.

## RESULTS

### The Orphan and Hongyan characteristics

To measure the morphological and biochemical fruit quality, the Orphan cultivar had a golden yellow peel colour, and Hongyan had an appealing bright red colour in phase III (Figure 1A). They exhibited similar fruit weights, soluble solids, titratable acid contents and peel thickness (Figure 1B–E, $P > 0.05$); however, Hongyan had approximately a 6 times higher anthocyanin content than Orphan (Figure 1F, $P < 0.05$).

**Analysis of the differentially expressed genes (DEGs).** To verify the changes at the genetic level, a high-throughput RNA-Seq was performed. Approximately 50 million clean reads were acquired from each sample with a Q30 percentage over 89% (Table 1) and assembled into 71 579 unigenes (Table 2). The unigenes were then annotated using BLASTX searches against the NCBI Nr protein sequence, SwissProt, EuKaryotic Orthologous Groups (KOG), and Kyoto Encyclopedia of Genes and Genomes (KEGG) databases. Among these unigenes, 3 028 were identified as being upregulated and 1 987 were down regulated based on an FDR ≤ 0.05 and log2 FC ≥ 1 (Figure 2A).

A qRT-PCR analysis was performed to verify the results from our RNA-seq data, and a total of 15 genes with different FPKMs were selected in Orphan and Hongyan (Figure 2D). Our results indicated that there was a high correlation coefficient between our transcriptome and the PCR results (Figure 2E).

A KEGG analysis was then performed using our transcriptional data, and the top three enriched pathways were tyrosine metabolism, phenylalanine

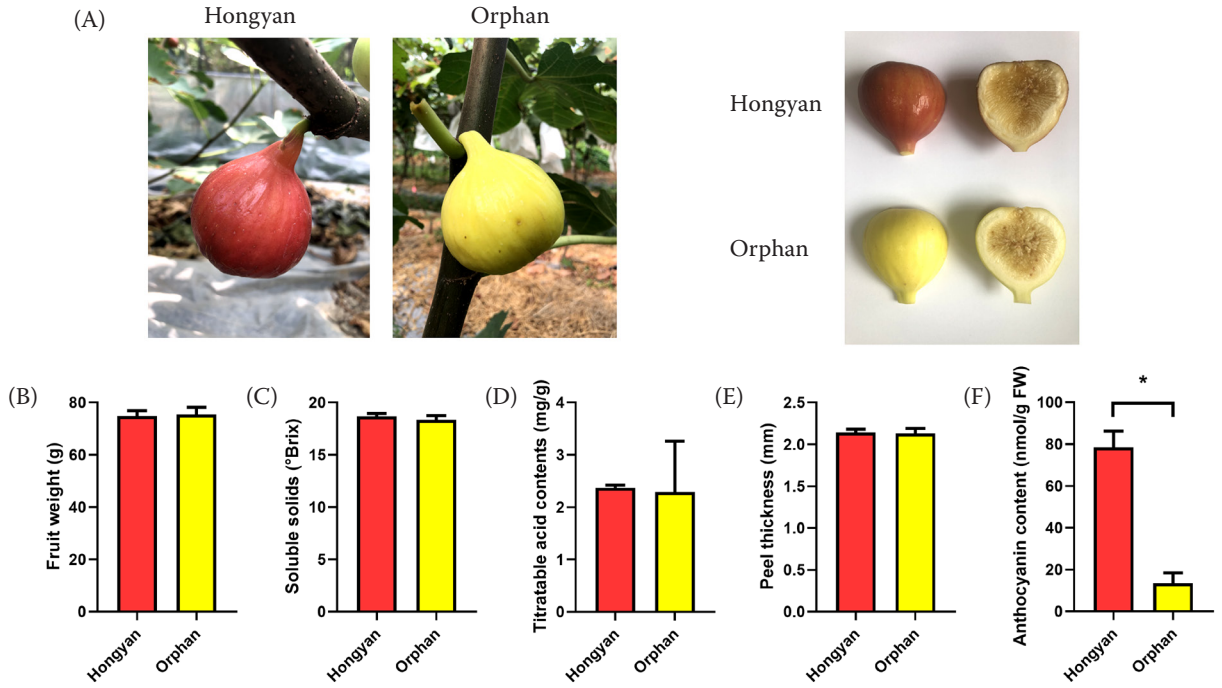


Figure 1. The characteristics of the fig *Ficus carica* L. cultivar Orphan and its red mutant cultivar Hongyan at phase III: the appearance of two fig fruits (A), fresh fruit weight (B), soluble solids (C), titratable acid contents (D), peel thickness (E) and anthocyanin content of the two figs (F)

Data are presented as the mean ± standard deviation (SD) of of three replicates, *significantly different at $P \leq 0.05$, Student's *t*-test; °Brix – degrees Brix; FW – fresh weight

https://doi.org/10.17221/42/2022-CJGPB

Table 1. Sequencing output of the transcriptome

| Samples | Total raw reads | Total clean reads | Total clean nucleotides | Q30 | GC |
|---|---|---|---|---|---|
| | | | | (%) | |
| H_1 | 49 940 622 | 47 816 288 | 7 172 443 200 | 90.99 | 47.43 |
| H_2 | 51 252 684 | 49 305 464 | 7 395 819 600 | 89.62 | 47.44 |
| H_3 | 50 285 854 | 48 232 930 | 7 234 939 500 | 90.77 | 47.38 |
| O_1 | 49 578 286 | 47 541 582 | 7 131 237 300 | 90.29 | 47.44 |
| O_2 | 52 150 672 | 49 873 198 | 7 480 979 700 | 91.21 | 47.31 |
| O_3 | 48 778 066 | 46 731 230 | 7 009 684 500 | 91.23 | 47.25 |

H – Hongyan; O – Orphan; Q30 – probability of an incorrect base call 1 in 1 000 times; GC – the percentage of G and C bases out of the total number of bases

metabolism, and isoquinoline alkaloid biosynthesis (Figure S1A in the ESM).

**Identification of the different abundance proteins (DAPs) in Orphan and its bud mutant Hongyan.** A total of 26 658 unique peptides were identified, and 5 535 proteins were annotated. The DAPs (Hongyan vs. Orphan) were identified according to a threshold of FC ≥ 1.5 or ≤ 0.67 and $P \leq 0.05$. Compared with Orphan, there were 109 upregulated and 53 downregulated proteins in Hongyan (Figure 2A). Our results for the KEGG analysis showed three enriched pathways: protein processing in the endoplasmic reticulum, ribosome, and flavonoid biosynthesis (Figure S1B in the ESM).

## Comparative analysis of the proteome and transcriptome

To analyse the consistency in the two omics between the two fig cultivars, the quantitative data for the DAPs and DEGs was analysed, and the result shown in Figure 2B indicate a poor correlation ($R = 0.01$) between the transcriptome and proteome results. The poor correlation of the results may emanate from the inconsistency in the transcription and translation over space and time and with the post-transcriptional regulation.

The DAPs and DEGs between Orphan and its bud mutant Hongyan were then compared to obtain insight into the relationship between the transcript levels and the protein abundance. A total of 15 DAPs and their cognate transcripts were upregulated in Hongyan, and two DAPs and their cognate transcripts were downregulated in Hongyan (Figure 2C). In addition, for 45 and 81 DAPs that were downregulated and upregulated, respectively, the cognate transcripts were unchanged. Six DAPs were downregulated while their cognate transcripts were upregulated, and 13 DAPs were upregulated while their cog-

Table 2. Statistics of the transcriptome

| | Sample | Total No. | Nucleotides | | N50 | Total consensus sequences |
|---|---|---|---|---|---|---|
| | | | total length | mean length | | |
| Contig | H_1 | 89 118 | 38 516 780 | 432 | 1 007 | – |
| | H_2 | 91 116 | 39 125 557 | 429 | 995 | – |
| | H_3 | 89 598 | 38 764 511 | 433 | 991 | – |
| | O_1 | 92 659 | 40 101 259 | 433 | 1 007 | – |
| | O_2 | 47 451 | 22 424 032 | 473 | 1 051 | – |
| | O_3 | 91 687 | 40 156 950 | 438 | 1 017 | – |
| Unigene | H_1 | 67 710 | 57 044 793 | 842 | 1 696 | 67 710 |
| | H_2 | 69 758 | 58 987 148 | 846 | 1 704 | 69 758 |
| | H_3 | 68 689 | 58 222 080 | 848 | 1 687 | 68 689 |
| | O_1 | 70 452 | 60 905 698 | 864 | 1 732 | 70 452 |
| | O_2 | 37 195 | 27 366 481 | 736 | 1 399 | 37 195 |
| | O_3 | 70 153 | 60 534 700 | 863 | 1 715 | 70 153 |

H – Hongyan; O – Orphan; N50 – the sequence length of the shortest contig/unigene at 50% of the total assembly length

https://doi.org/10.17221/42/2022-CJGPB

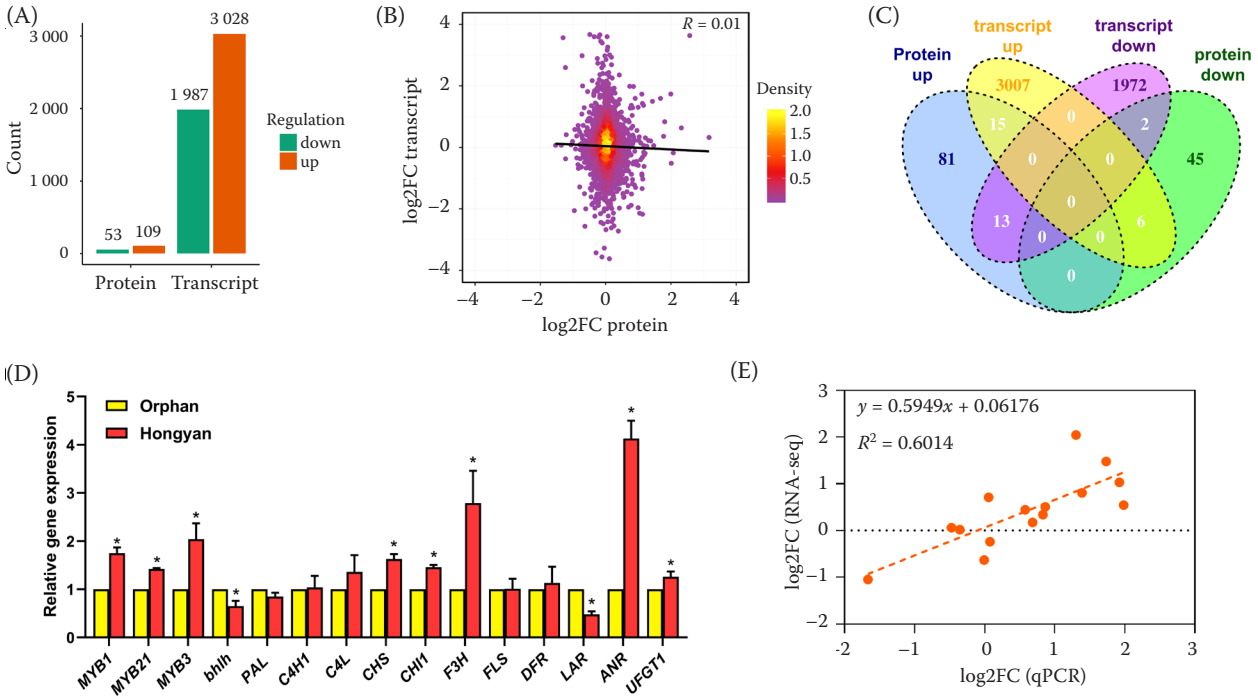


Figure 2. The general profiles of the transcriptome and proteome: the differentially expressed genes (DEGs) and different abundance proteins (DAPs)in the two fig cultivars (A), correlation analysis of the overall proteome and transcriptome of two the fig cultivars (B), Venn diagram of the DEGs and DAPs (C), the real-time quantitative PCR detected the mRNA expression of the selected genes; data are presented as the mean ± SD of of three replicates, *significantly different at $P \leq 0.05$, Student's *t* test; FC – fold change (D), the RNA-Seq validation and correlation analysis by real-time quantitative PCR (E)

nate transcripts were downregulated. There were 164 and 216 DEGs observed to be downregulated and upregulated, respectively, while their cognate proteins remained unchanged (Figure 2C). A KEGG enrichment was conducted to classify the functions of the DAPs and DEGs, according to their different expression patterns. The 15 upregulated DAPs and their cognate DEGs were assigned to the flavonoid biosynthesis pathway. The 81 upregulated DAPs for which the cognate transcripts were unchanged were assigned to the phenylpropanoid biosynthesis, flavonoid biosynthesis, plant hormone signal transduction, stilbenoid, diarylheptanoid and gingerol biosynthesis and phenylalanine, tyrosine and tryptophan biosynthesis pathways. Thirteen upregulated DAPs with downregulated cognate transcripts in Hongyan were assigned to the protein processing in the endoplasmic reticulum pathway. The DEGs that were upregulated while their cognate proteins were unchanged were assigned to the phenylpropanoid biosynthesis, monoterpenoid biosynthesis and photosynthesis pathways. The 164 DEGs that were solely downregulated at the transcription level were enriched in six KEGG pathways: alanine, aspartate and glutamate metabolism, base excision repair, nitrogen metabolism, pentose and glucuronate interconversions, RNA degradation, and taurine and hypotaurine metabolism. Forty-five DAPs were downregulated only at the protein level and were assigned to the ribosome pathway (Figure 3), these results reflected the changes in the gene and protein expression between the two fig cultivars and identified two pathways significantly upregulated in Hongyan, the phenylpropanoid biosynthesis and flavonoid biosynthesis, which may contribute to the red colour formation. To further analyse the underlying potential mechanism involved in the fig colouration, some candidate transcripts and cognate proteins, according to their different expression patterns, are listed in Table 3. Several upregulated proteins in Hongyan with potential biological functions participated in the biosynthesis of anthocyanin. Feruloyl CoA ortho-hydroxylase 1-like (FCH 1-like, Unigene29179_All) and C4H (CL6895.Contig1_All) were involved in the phenylpropanoid biosynthesis and were upregulated at the protein level, but not at the transcriptional level. Additionally, C4H (CL6895.Contig1_All) participated in the flavonoid

https://doi.org/10.17221/42/2022-CJGPB

Table 3. Pathways associated with the candidate different abundance proteins (DAPs) and differentially expressed genes (DEGs) between the two fig cultivars

| Protein-transcript express pattern | Gene ID | Annotation | Log2FC-protein | *P*-value | Log2FC-transcript | *P*-value |
|---|---|---|---|---|---|---|
| **Up-down** | | | | | | |
| gmx04141 protein processing in endoplasmic reticulum | CL1838.Contig2_All | 15.7 kDa heat shock protein, peroxisomal-like | 0.59 | 1.53E-05 | –1.13 | 3.05E-02 |
| | Unigene815_All | heat-shock protein, putative | 0.65 | 2.42E-04 | –1.44 | 3.33E-03 |
| | Unigene832_All | ER-localised small heat-shock protein | 0.70 | 6.23E-04 | –1.94 | 2.06E-04 |
| | Unigene2020_All | class II small heat shock protein Le-HSP17.6 | 1.04 | 1.44E-04 | –2.14 | 1.25E-02 |
| | Unigene28410_All | predicted protein | 0.79 | 1.06E-03 | –1.52 | 5.08E-05 |
| | Unigene8110_All | 22.0 kDa class IV heat shock protein | 1.00 | 3.99E-04 | –1.96 | 8.95E-05 |
| | CL496.Contig1_All | full = 17.5 kDa class I heat shock protein | 0.82 | 1.76E-03 | –1.18 | 9.37E-03 |
| **Up-unchanged** | | | | | | |
| gmx00940 phenylpropanoid biosynthesis | Unigene29179_All | feruloyl CoA ortho-hydroxylase 1-like | 0.67 | 1.96E-03 | –0.59 | 1.21E-04 |
| | CL6895.Contig1_All | cinnamate 4-hydroxylase, putative | 0.86 | 2.61E-04 | –0.47 | 4.56E-04 |
| gmx00941 flavonoid biosynthesis | CL6991.Contig1_All | dihydroflavonol 4-reductase | 0.83 | 1.21E-04 | 0.69 | 8.25E-05 |
| | CL1001.Contig1_All | Chalcone synthase | 1.17 | 7.00E-04 | 0.06 | 7.06E-01 |
| | CL6895.Contig1_All | cinnamate 4-hydroxylase, putative | 0.86 | 2.61E-04 | –0.47 | 4.56E-04 |
| | Unigene17768_All | UDP-glucose: flavonoid 3-O-glucosyltransferase | 1.81 | 4.48E-06 | 0.83 | 3.17E-02 |
| gmx00400 phenylalanine, tyrosine and tryptophan biosynthesis | Unigene1165_All | phospho-2-dehydro-3-deoxyheptonate aldolase 2, chloroplastic-like | 0.86 | 3.00E-03 | 0.35 | 1.02E-02 |
| | CL2377.Contig1_All | phospho-2-dehydro-3-deoxyheptonate aldolase 2 | 0.61 | 2.24E-04 | 0.20 | 7.18E-03 |
| **Up-up** | | | | | | |
| gmx00941 flavonoid biosynthesis | Unigene27661_All | flavanone-3-hydroxylase | 2.00 | 3.84E-04 | 1.74 | 5.47E-05 |
| | Unigene21588_All | chalcone isomerase | 0.74 | 5.73E-05 | 1.98 | 6.66E-05 |
| | Unigene19670_All | anthocyanin synthase | 2.15 | 2.47E-05 | 6.84 | 1.76E-05 |
| | Unigene7902_All | anthocyanidin reductase | 0.99 | 1.54E-03 | 1.30 | 1.46E-05 |
| **Down-unchanged** | | | | | | |
| gmx03010 ribosome | CL6290.Contig2_All | cytoplasmic ribosomal protein S13-like | –0.68 | 8.68E-03 | 0.01 | 1.00E+00 |
| | Unigene21741_All | 60S ribosomal protein L13aA | –0.72 | 3.97E-04 | –0.03 | 9.28E-01 |
| | CL7071.Contig2_All | 60S ribosomal protein L7-4 | –0.63 | 9.99E-05 | –0.01 | 1.00E+00 |
| | Unigene31874_All | 60S ribosomal protein L27-like | –0.73 | 2.84E-03 | 0.38 | 3.85E-02 |
| | CL7648.Contig2_All | 40S ribosomal protein S4-3 | –0.72 | 1.17E-04 | –0.07 | 6.00E-01 |
| | Unigene1344_All | 60S ribosomal protein L35-like | –0.73 | 2.97E-04 | 0.13 | 1.76E-01 |

https://doi.org/10.17221/42/2022-CJGPB

Table 3 to be continued

| Protein-transcript express pattern | Gene ID | Annotation | Log2FC-protein | *P*-value | Log2FC-transcript | *P*-value |
|---|---|---|---|---|---|---|
| **Down-unchanged** | | | | | | |
| gmx03010 ribosome | Unigene25353_All | Os01g0304000, chain d, localization of the large subunit ribosomal proteins into A 5.5 A Cryo-Em map of *Triticum aestivum* translating 80 s ribosome | –0.59 | 7.98E-04 | 0.20 | 3.23E-01 |
| | CL7648.Contig1_All | 40S ribosomal protein S4-like | –0.71 | 9.83E-04 | 0.00 | 1.00E+00 |
| | CL6290.Contig1_All | 40S ribosomal protein S13, putative | –0.78 | 7.80E-05 | –0.08 | 7.25E-01 |
| **Down-down** | | | | | | |
| | CL1144.Contig1_All | thaumatin-like protein | –0.80 | 5.62E-04 | –1.29 | 4.05E-03 |
| | CL3314.Contig2_All | subtilisin-like protease | –0.96 | 6.34E-03 | –2.06 | 1.95E-02 |

biosynthesis as well as CHS (CL1001.Contig1_All), DFR (CL6991.Contig1_All), C4H (CL6895.Contig1_All), and UGFT (Unigene17768_All), with upregulation only detected at the protein level. Another two candidates, phospho-2-dehydro-3-deoxyheptonate aldolase 2, chloroplastic-like (Unigene1165_All) and phospho-2-dehydro-3-deoxyheptonate aldolase 2 (CL2377.Contig1_All), which were only upregulated at the protein level, were functionally classified into phenylalanine, tyrosine and tryptophan biosynthesis. Additionally, four genes upregulated at both the protein and transcriptional levels were included in the flavonoid biosynthesis: F3H (Unigene27661_All), CHI (Unigene21588_All), ANS (Unigene19670_All), and ANR (Unigene7902_All). In addition, several heat shock proteins were also upregulated at the protein level, but downregulated at the transcript level, including CL1838.Contig2_All, Unigene815_All, Unigene832_All, Unigene2020_All, Unigene28410_All, Unigene8110_All and CL496.Contig1_All, which were assigned to the protein processing in the endoplasmic reticulum.

## DISCUSSION

The peel colour is an important characteristic of fruits (Aljane et al. 2020). Thus, gaining insight into the fruit peel colouration at the genetic level

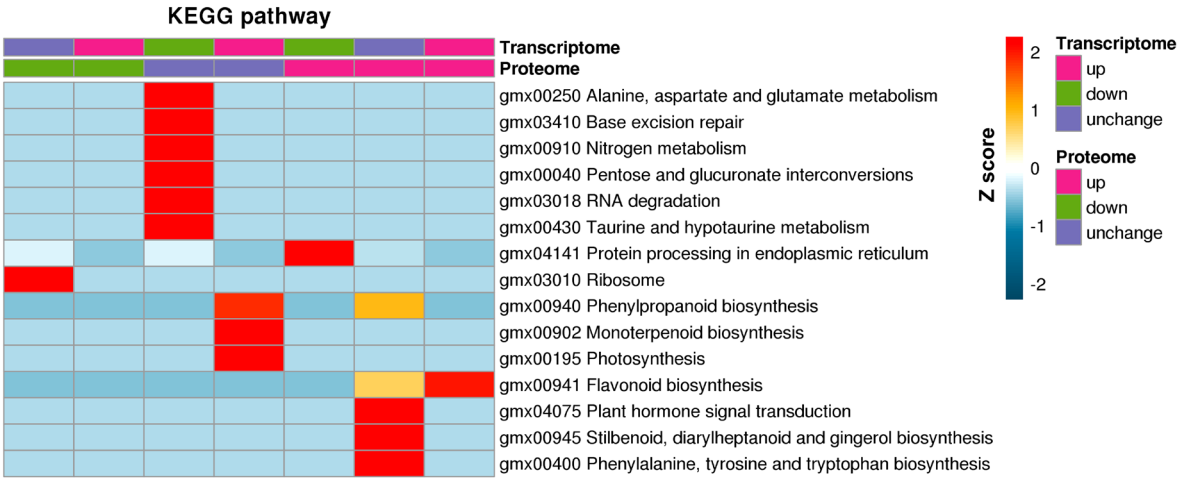


Figure 3. Significant enrichment analysis of the differentially expressed genes (DEGs) for each pair of protein and cognate mRNAs based on the direction of the change; KEGG – Kyoto Encyclopedia of Genes and Genomes

https://doi.org/10.17221/42/2022-CJGPB

is important for the selection of new cultivars. Figs with a dark colour, e.g., red, purple and black, always contain high levels of anthocyanins, which play a primary role in the fruit colouration (Treutter 2005; Page et al. 2012).

The comparative analysis between the proteome and transcriptome revealed that only a small portion of the proteins and their cognate transcripts exhibited similar variation tendencies in Orphan with its yellow fruit peel and Hongyan, which is a bud mutant of Orphan. This expression inconsistency may result from the post-translational modifications and splicing events, or the quick fluctuation of the transcription (Luo et al. 2018). Besides, we sampled the fig fruits at the middle of phase III, at this time point, however, the colouration is nearly completed. We speculated that the figs in this phase have weaker biological processes, e.g., transcription and translation, and some early transcription factors for anthocyanin biosynthesis are not active.

In our current study, some DEGs and DAPs involved in the anthocyanin biosynthesis were concluded (Figure 4), a majority of the participants were found to be upregulated in the protein and mRNA level, except for PAL, C4L and F3'H. While we failed to find the consistent expression pattern of some transcription factors in two omics, e.g., MYBs, bHLHs or WRKYs, despite a large number of them being identified as differently expressed in the transcription level, their proteins remain unchanged. The variation in the phenotype might largely be behind the gene expression, a similar conclusion can apply to the protein abundance (Wang et al. 2017). Besides, the time we sampled for the fig fruit (phase III, nearly ripe) might also attribute to the fruits missing these transcription factors, fruits in phase II or earlier might be more suitable for the investigation of the molecular basis in the mutation, which deserves further study.

Several upregulated DAPs with downregulated cognate transcripts in Hongyan were assigned to the protein processing in the endoplasmic reticulum (Table 3). Some of these DAPs were annotated as heat shock proteins. Heat shock proteins were first shown to respond to heat stimulation, to prevent protein misfolding and aggregation (Lindquist & Craig 1988; Young et al. 2001). Heat shock proteins play critical roles in the phenomena related to the biotic and abiotic defence, such as thermotolerance (Queitsch et al. 2000), pathogen defence (Gorovits et al. 2013), drought tolerance (Sato & Yokoya 2008), and chilling tolerance (Sabehat et al. 1996). The upregulation of the heat shock proteins identified in Hongyan may imply a possible phenotypic difference in the biotic and abiotic resistance of the red peel mutant.

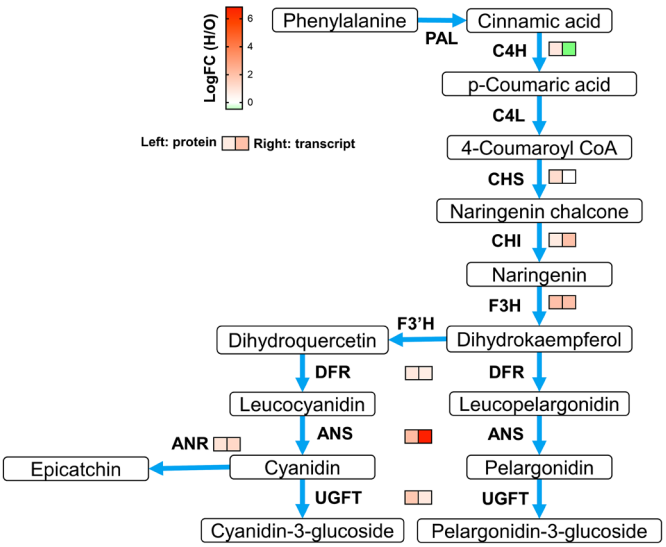


Figure 4. Comparative analysis of the transcripts and proteins involved in the anthocyanin biosynthesis in two fig cultivars
PAL – phenylalanine ammonia-lyase; C4H – cinnamic acid 4-hydroxylase; 4CL – 4-coumarate CoA ligase; CHS – chalcone synthase; CHI – chalcone isomerase; F3H – flavanone 3-hydroxylase; F3'H – flavanoid 3'-hydroxylase; DFR – dihydroflavonol 4-reductase; FR – flavanone 4-reductase; ANS/LDOX – anthocyanidin synthase/leucocyanidin oxygenase; UFGT – UDP glucose-flavonoid 3-O-glcosyl-transferase; FLS – flavonol synthesis; LAR – leucocyanidin reductase; ANR – anthocyanin reductase

https://doi.org/10.17221/42/2022-CJGPB

## CONCLUSION

Our results in the transcriptome and proteome analysis illustrated a transcriptional and translational network in the peel colour formation in the figs. The primary variation between Orphan and its red peel mutant in phase III is identified as the anthocyanin biosynthesis, a large portion of the enzymes promoting the pathway were upregulated in the red mutant, both on the transcription and protein level. These candidate DAPs and DEGs obtained by integrative transcriptome and proteome analysis may be critical for illustrating the genetic basis for the formation of the colour mutant, and provide new insight into fig breeding.

## REFERENCES

Aljane F., Neily M.H., Msaddak A. (2020): Phytochemical characteristics and antioxidant activity of several fig (*Ficus carica* L.) ecotypes. Italian Journal of Food Science, 32: 755–768.

Allan A.C., Hellens R.P., Laing W.A. (2008): MYB transcription factors that colour our fruit. Trends in Plant Science, 13: 99–102.

Bradford M.M. (1976): A rapid and sensitive method for the quantitation of microgram quantities of protein utilizing the principle of protein-dye binding. Analytical Biochemistry, 72: 248–254.

Chai L., Li Y., Chen S., Perl A., Zhao F., Ma H. (2014): RNA sequencing reveals high resolution expression change of major plant hormone pathway genes after young seedless grape berries treated with gibberellin. Plant Science, 229: 215–224.

Crisosto C.H., Bremer V., Ferguson L., Crisosto G.M. (2010): Evaluating quality attributes of four fresh fig (*Ficus carica* L.) cultivars harvested at two maturity stages. HortScience, 45: 707–710.

Dueñas M., Pérez-Alonso J.J., Santos-Buelga C., Escribano-Bailón T. (2008): Anthocyanin composition in fig (*Ficus carica* L.). Journal of Food Composition and Analysis, 21: 107–115.

Fiddler L., Hecht L., Nelson E.E., Nelson E.N., Ross J. (2011): SPSS for Windows 16.0: A Basic Tutorial. Social Science Research and Instruction Center. California State University.

Gorovits R., Moshe A., Ghanim M., Czosnek H. (2013): Recruitment of the host plant heat shock protein 70 by Tomato yellow leaf curl virus coat protein is required for virus infection. PLoS ONE, 8: e70280.

Gowd V., Jia Z., Chen W. (2017): Anthocyanins as promising molecules and dietary bioactive components against diabetes – A review of recent advances. Trends in Food Science and Technology, 68: 1–13.

Höll J., Vannozzi A., Czemmel S., D'Onofrio C., Walker A.R., Rausch T., Lucchin M., Boss P.K., Dry I.B., Bogs J. (2013): The R2R3-MYB transcription factors MYB14 and MYB15 regulate stilbene biosynthesis in *Vitis vinifera*. Plant Cell, 25: 4135–4149.

Khadari B., Lashermes P., Kjellberg F. (1995): RAPD fingerprints for identification and genetic characterization of fig (*Ficus carica* L.) genotypes. Journal of Genetics and Breeding, 49: 77–77.

Kislev M.E., Hartmann A., Bar-Yosef O. (2006): Early domesticated fig in the Jordan Valley. Science, 312: 1372–1374.

Lindquist S., Craig E.A. (1988): The heat-shock proteins. Annual Review of Genetics, 22: 631–677.

Luo X., Cao D., Li H., Zhao D., Xue H., Niu J., Chen L., Zhang F., Cao S. (2018): Complementary iTRAQ-based proteomic and RNA sequencing-based transcriptomic analyses reveal a complex network regulating pomegranate (*Punica granatum* L.) fruit peel colour. Scientific Reports, 8: 1–13.

Marei N., Crane J.C. (1971): Growth and respiratory response of fig (*Ficus carica* L. cv. Mission) fruits to ethylene. Plant Physiology, 48: 249–254.

Mori K., Shirasawa K., Nogata H., Hirata C., Tashiro K., Habu T., Kim S., Himeno S., Kuhara S., Ikegami H. (2017): Identification of RAN1 orthologue associated with sex determination through whole genome sequencing analysis in fig (*Ficus carica* L.). Scientific Reports, 7: 41124.

Page M., Sultana N., Paszkiewicz K., Florance H., Smirnoff N. (2012): The influence of ascorbate on anthocyanin accumulation during high light acclimation in *Arabidopsis thaliana*: Further evidence for redox control of anthocyanin synthesis. Plant, Cell and Environment, 35: 388–404.

Pascual-Teresa D., Moreno D.A., García-Viguera C. (2010): Flavanols and anthocyanins in cardiovascular health: A review of current evidence. International Journal of Molecular Sciences, 11: 1679–1703.

Queitsch C., Hong S.-W., Vierling E., Lindquist S. (2000): Heat shock protein 101 plays a crucial role in thermotolerance in *Arabidopsis*. Plant Cell, 12: 479–492.

Sabehat A., Weiss D., Lurie S. (1996): The correlation between heat-shock protein accumulation and persistence and chilling tolerance in tomato fruit. Plant Physiology, 110: 531–537.

Sato Y., Yokoya S. (2008): Enhanced tolerance to drought stress in transgenic rice plants overexpressing a small heat-shock protein, sHSP17. 7. Plant Cell Reports, 27: 329–334.

Solomon A., Golubowicz S., Yablowicz Z., Grossman S., Bergman M., Gottlieb H.E., Altman A., Kerem Z., Flaish-

https://doi.org/10.17221/42/2022-CJGPB

man M.A. (2006a): Antioxidant activities and anthocyanin content of fresh fruits of common fig (*Ficus carica* L.). Journal of Agricultural and Food Chemistry, 54: 7717–7723.

Tanaka Y., Sasaki N., Ohmiya A. (2008): Biosynthesis of plant pigments: Anthocyanins, betalains and carotenoids. Plant Journal, 54: 733–749.

Treutter D. (2005): Significance of flavonoids in plant resistance and enhancement of their biosynthesis. Plant Biology, 7: 581–591.

Wang B., He J., Bai Y., Yu X., Li J., Zhang C., Xu W., Bai X., Cao X., Wang S. (2013): Root restriction affected anthocyanin composition and up-regulated the transcription of their biosynthetic genes during berry development in 'Summer Black'grape. Acta Physiologiae Plantarum, 35: 2205–2217.

Wang Z., Cui Y., Vainstein A., Chen S., Ma H. (2017): Regulation of fig (*Ficus carica* L.) fruit color: Metabolomic and transcriptomic analyses of the flavonoid biosynthetic pathway. Frontiers in Plant Science, 8: 1990.

Wei L., Cao Y., Cheng J., Xiang J., Shen B., Wu J. (2020): Comparative transcriptome analyses of a table grape 'Summer Black' and its early-ripening mutant 'Tiangong Moyu' identify candidate genes potentially involved in berry development and ripening. Journal of Plant Interactions, 15: 213–222.

Young J.C., Moarefi I., Hartl F.U. (2001): Hsp90: A specialized but essential protein-folding tool. Journal of Cell Biology, 154: 267.

Zhao X., Li W.-F., Wang Y., Ma Z.-H., Yang S.-J., Zhou Q., Mao J., Chen B.-H. (2019): Elevated $CO_2$ concentration promotes photosynthesis of grape (*Vitis vinifera* L. cv. 'Pinot noir') plantlet in vitro by regulating RbcS and Rca revealed by proteomic and transcriptomic profiles. BMC Plant Biology, 19: 1–16.

Received: May 26, 2022
Accepted: August 31, 2022
Published online: October 6, 2022